

Context

Thanks to the discovery by Fermi/LAT of nearly sixty new gamma-ray pulsars (Abdo et al. 2010), it becomes possible to look for statistical properties of their pulsed high-energy emission, light-curves and spectra. These pulsars emit by definition mostly gamma-ray photons but some of them are also detected in the radio band. For those seen in these two extreme energies, the relation between time lag of radio/gamma-ray pulses and gamma-ray peak separation helps to put some constrain on the magnetospheric emission mechanisms and location.

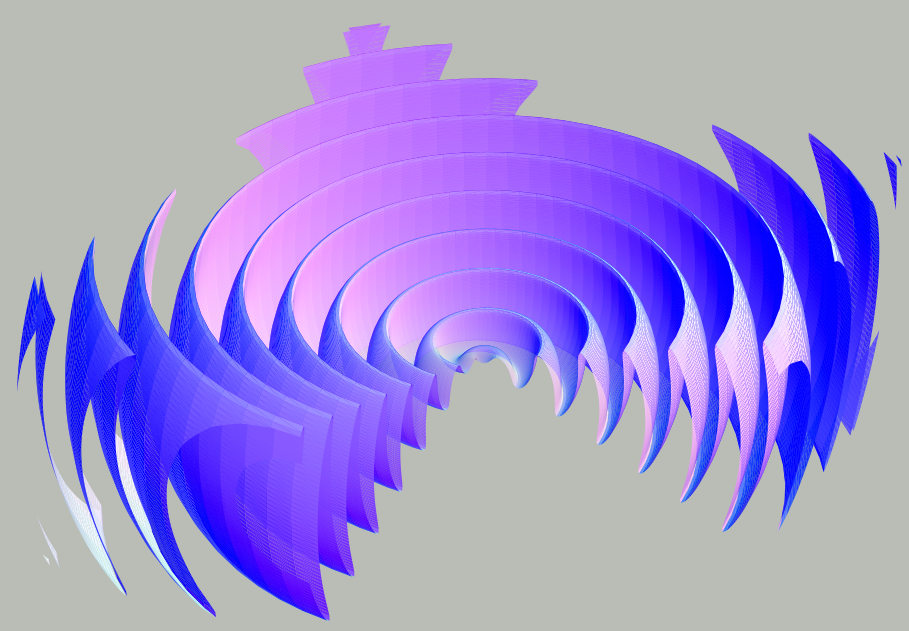
Method

This idea is analyzed in detail here, assuming

- ▶ a polar cap model for the radio pulses
- ▶ the striped wind geometry for the pulsed high-energy counterpart.

Combining the time-dependent emissivity in the wind, supposed to be inverse Compton radiation, with a simple polar cap emission model along and around the magnetic axis, we compute the radio and gamma-ray light-curves, summarizing the results in several phase plots.

Polar cap/stripped wind model



Parameters of the model [Pétri (2009)]

- ▶ magnetic obliquity χ
- ▶ inclination of the line of sight ζ
- ▶ current sheet thickness Δ_φ
- ▶ particle density number contrast N/N_0
- ▶ polar cap emissivity = gaussian shape centered about the magnetic axis.

Figure: The striped pulsar wind.

The phase lag as well as the gamma-ray peak separation dependence on the pulsar inclination angle and on the viewing angle are studied. Using the gamma-ray pulsar catalog compiled from the Fermi data, we are able to predict the radio lag/peak separation relation and compare it with available observations taken from this catalog [Pétri (2011)].

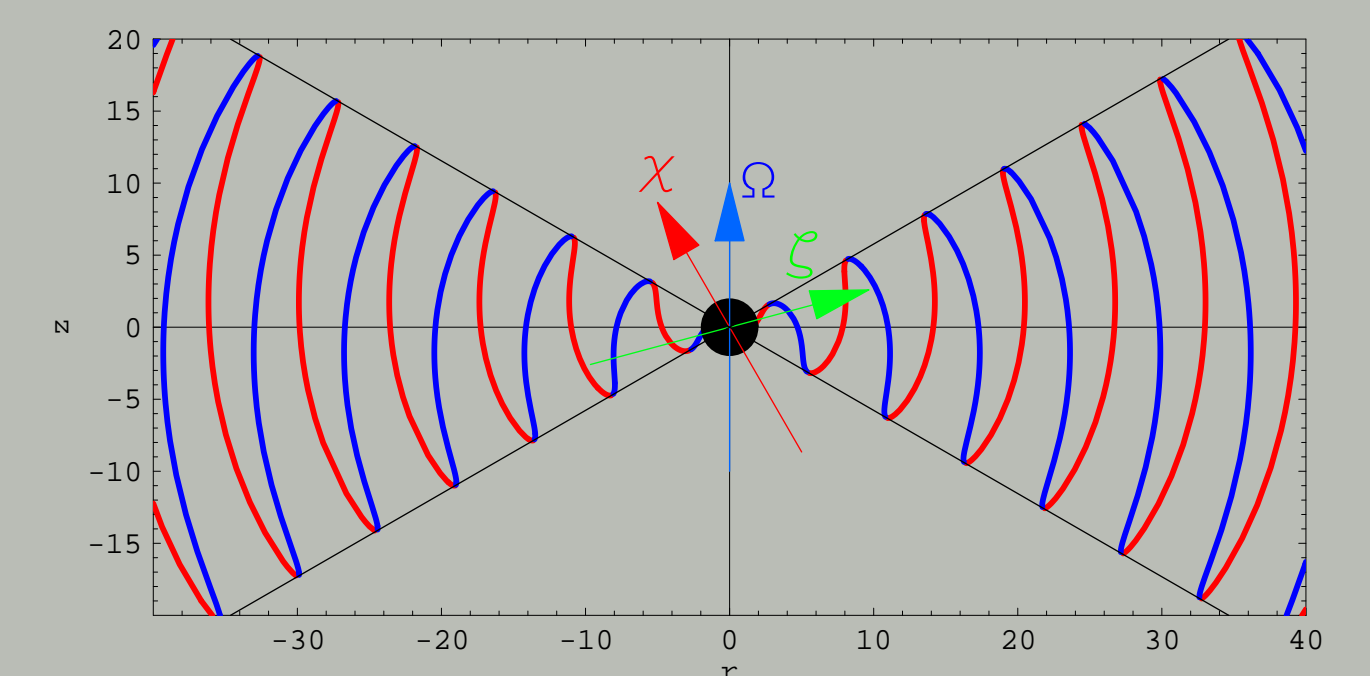


Figure: Geometry of the current sheet.

Phase plots

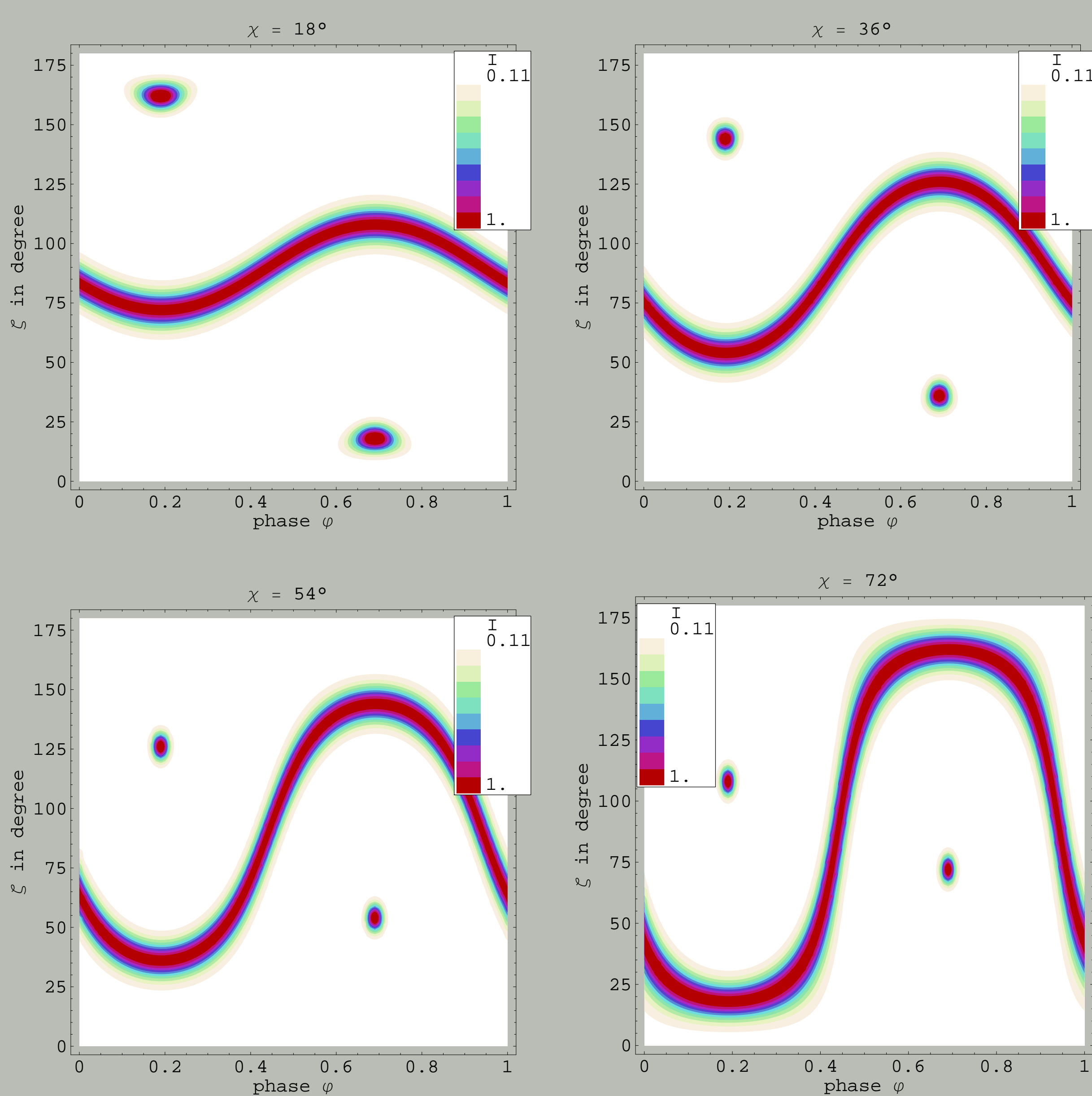


Figure: Phase plot of the pulsed gamma-ray and radio emission components for $\zeta \in [0^\circ, 180^\circ]$ and $\chi = 18^\circ, 36^\circ, 54^\circ, 72^\circ$.

Light-curves vs model parameters

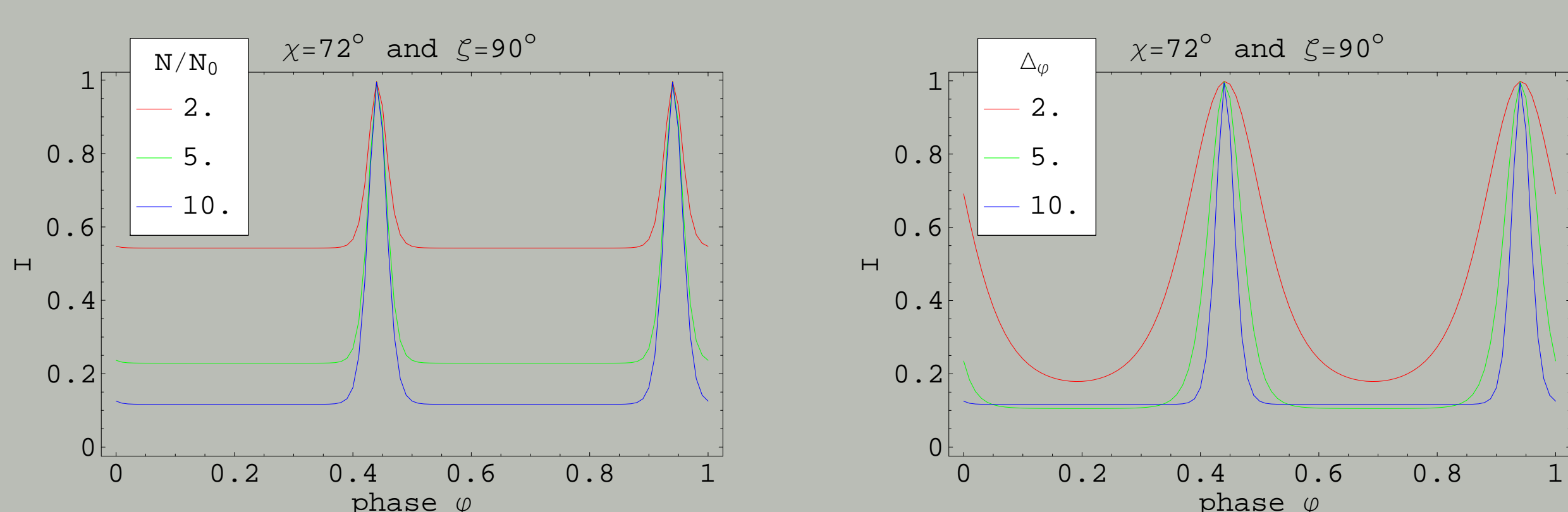


Figure: Light-curves of the pulsed gamma-ray emission component for $\zeta = 90^\circ$ and $\chi = 72^\circ$. On the left, for different contrast N/N_0 with $\Delta_\varphi = 10$ and on the right for different thickness Δ_φ with $N/N_0 = 10$.

Peak morphology vs pulsar geometry

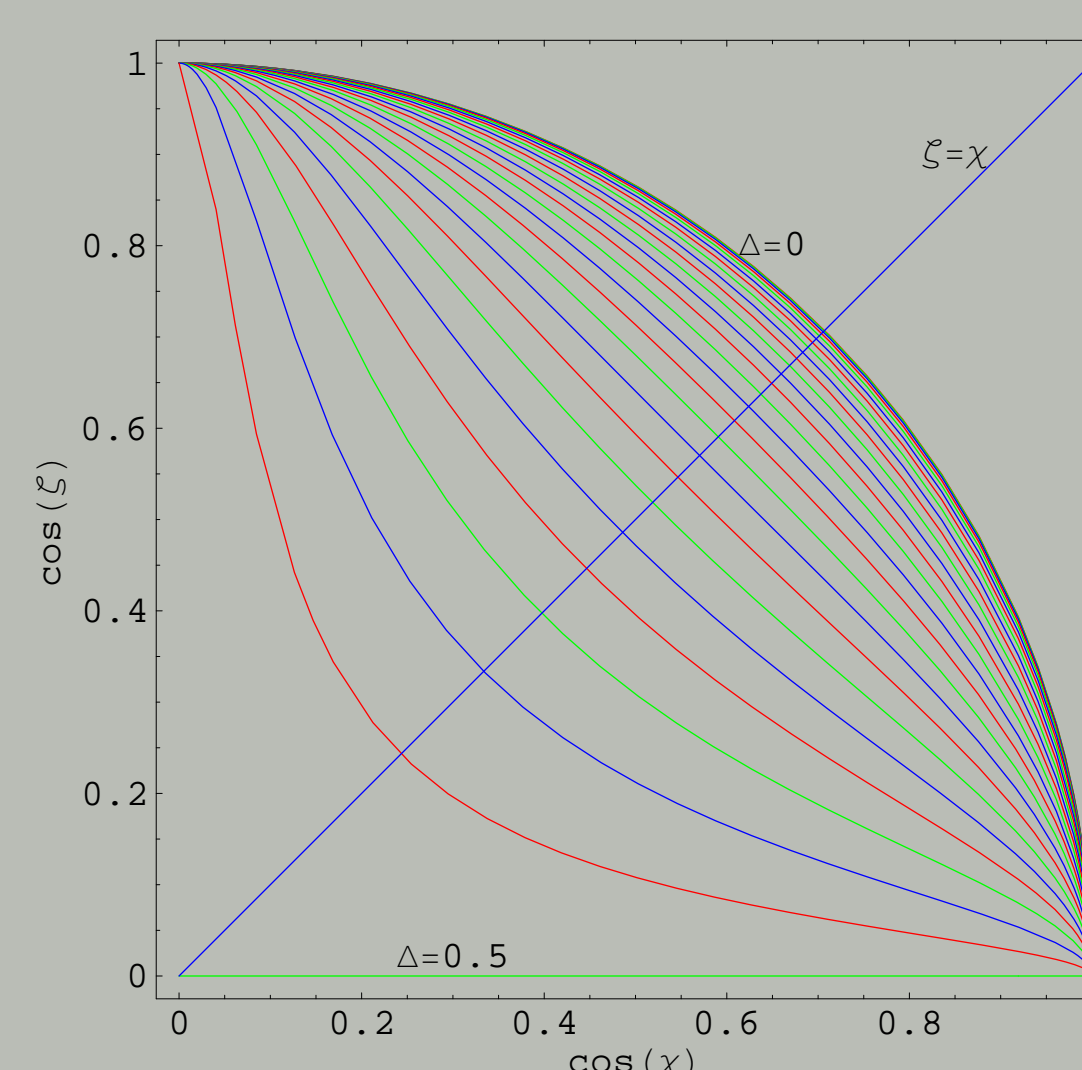


Figure: Peak separation Δ between both gamma-ray pulses vs obliquity χ and inclination angle of the line of sight ζ .

The gamma-ray peak separation Δ is related to the geometry according to the relation

$$\cos(\pi \Delta) = |\cot \zeta \cot \chi|$$

and shown on the left figure. Each curve represents a constant value of Δ ranging from 0 to 0.5 by 0.02 steps. No separation occurs along the circle of radius unity (pulse overlapping) whereas maximum separation of 0.5 is reached for $\cos \zeta = 0$. The diagonal $\zeta = \chi$ describes the visibility of one magnetic pole.

Gamma-ray peak separation vs radio time lag

The radio time lag δ is simply related to the gamma-ray peak separation Δ

$$\delta \approx \frac{1 - \Delta}{2} \quad (1)$$

This has to be compared with the $\delta - \Delta$ diagram published in [Abdo et al. (2010)] as shown on the right figure. All the points but one lie below the line given by Eq. (1). The spread in radio lag along this line can be understood as a fluctuation in the precise location of the most significant emission in the wind.

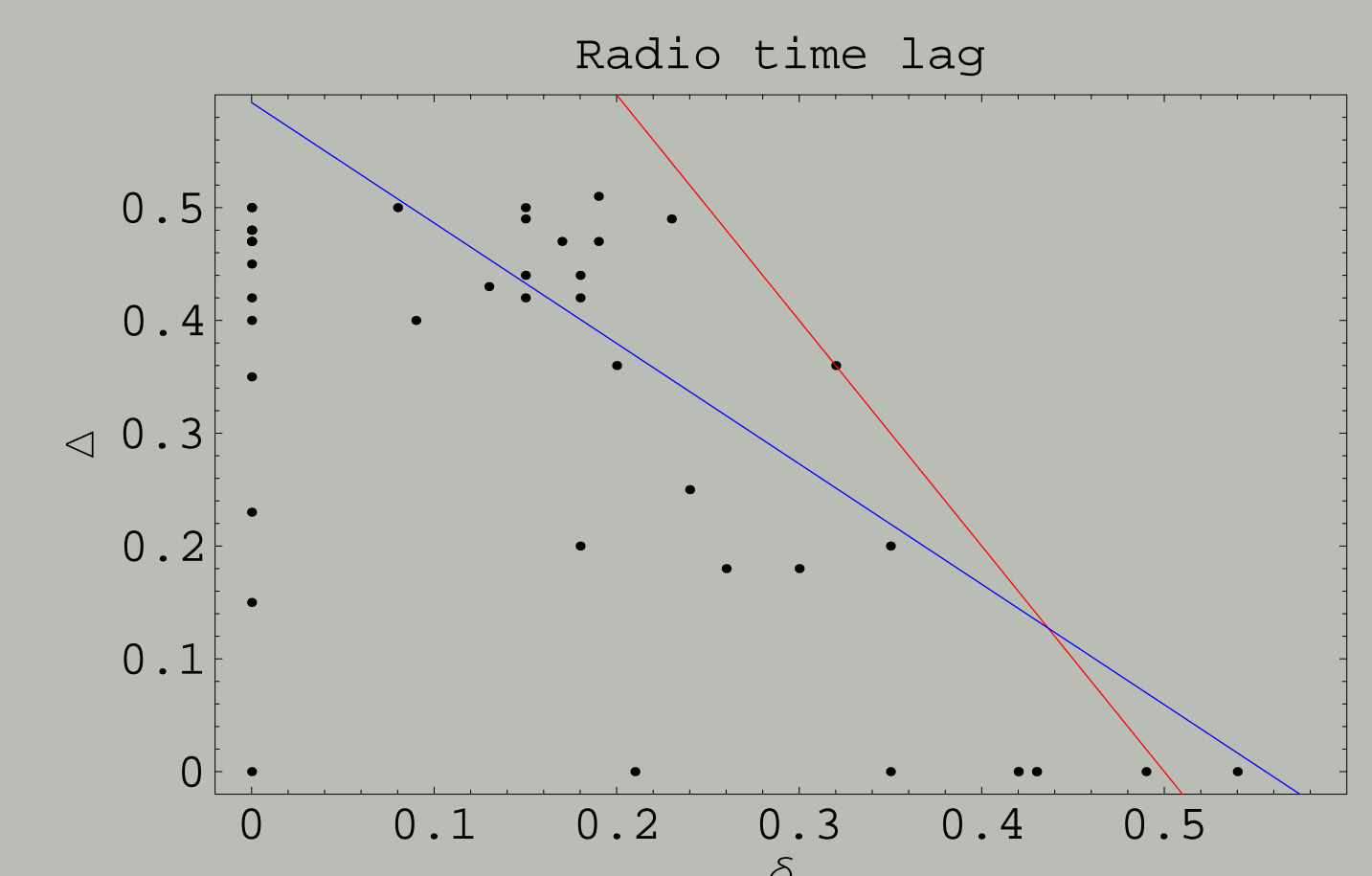


Figure: Gamma-ray peak separation Δ vs radio time lag δ as observed by Fermi-LAT (black dots). The blue curve is a linear fit and the red straight line the upper limit as predicted by Eq. (1).

Bibliography

- Abdo, A. A., et al. 2010, ApJS, 187, 460
- Pétri, J. 2009, A&A, 503, 13
- Pétri, J. 2011, MNRAS, 412, 1870